Sensing and Bio-Sensing Research 5 (2015) 13–18

Contents lists available at ScienceDirect

Sensing and Bio-Sensing Research

journal homepage: www.elsevier.com/locate/sbsr

Controlling "chemical nose" biosensor characteristics by modulating gold nanoparticle shape and concentration

Mohit S. Verma [a,b], Paul Z. Chen [a], Lyndon Jones [a,c], Frank X. Gu [a,b,*]

[a] Department of Chemical Engineering, University of Waterloo, 200 University Avenue W, Waterloo, Ontario N2L 3G1, Canada
[b] Waterloo Institute for Nanotechnology, University of Waterloo, 200 University Avenue W, Waterloo, Ontario N2L 3G1, Canada
[c] Centre for Contact Lens Research, University of Waterloo, 200 University Avenue W, Waterloo, Ontario N2L 3G1, Canada

ARTICLE INFO

Keywords:
Morphology
Color change
Staphylococcus aureus
Point-of-care
Nanocubes
Nanorods

ABSTRACT

Conventional lock-and-key biosensors often only detect a single pathogen because they incorporate biomolecules with high specificity. "Chemical nose" biosensors are overcoming this limitation and identifying multiple pathogens simultaneously by obtaining a unique set of responses for each pathogen of interest, but the number of pathogens that can be distinguished is limited by the number of responses obtained. Herein, we use a gold nanoparticle-based "chemical nose" to show that changing the shapes of nanoparticles can increase the number of responses available for analysis and expand the types of bacteria that can be identified. Using four shapes of nanoparticles (nanospheres, nanostars, nanocubes, and nanorods), we demonstrate that each shape provides a unique set of responses in the presence of different bacteria, which can be exploited for enhanced specificity of the biosensor. Additionally, the concentration of nanoparticles controls the detection limit of the biosensor, where a lower concentration provides better detection limit. Thus, here we lay a foundation for designing "chemical nose" biosensors and controlling their characteristics using gold nanoparticle morphology and concentration.

1. Introduction

"Chemical nose" biosensors are gaining considerable attention as a replacement to their conventional counterparts that often require biomolecules such as aptamers and antibodies [1-9]. A "chemical nose" has the ability to produce unique patterns in the presence of the analyte, which facilitate the identification of the analyte [10]. Gold nanoparticles have been implemented as a "chemical nose" biosensor for the detection of proteins [1,11], cancer cells [10,12], and bacteria [6,7].

A recent strategy for detecting bacteria using gold nanoparticles has been the use of electrostatic and hydrophobic interactions between bacterial cell walls and nanoparticle surfaces coated with cetyltrimethylammonium bromide (CTAB) [6,13]. This approach provides a versatile platform for applying gold nanoparticles for the detection, identification, and quantification of bacteria. In order to exploit the potential of a gold nanoparticle-based "chemical nose," an understanding of the parameters that control specificity and sensitivity are necessary, but to-date are not well-understood. Here, we show that controlling the shape and concentration of gold nanoparticles determines the specificity and sensitivity of the "chemical nose" biosensor. We used four gold nanoparticle shapes: nanospheres, nanostars, nanocubes, and nanorods to detect two Gram-positive (*Staphylococcus aureus* and *Enterococcus faecalis*) and two Gram-negative (*Escherichia coli* and *Pseudomonas aeruginosa*) bacteria. These bacteria are notorious for contaminating food, water, and hospital surfaces and for leading to antibiotic resistant infections [14]. Detection and identification of these bacteria at the point-of-care using a "chemical nose" biosensor will help to prevent such infections.

2. Materials and methods

Gold nanoparticles were synthesized using previously published methods [6,13,15,16], and kept in 1 mM CTAB, except for gold nanorods, which were purchased from Nanopartz Inc. (Loveland, CO, United States) and used without purification. The shapes of nanoparticles were verified using transmission electron microscopy (TEM). The methods were chosen such that each nanoparticle shape would be approximately similar in size (~40–60 nm). Bacteria were cultured, washed, and normalized to an optical density at 660 nm (OD_{660nm}) of 0.1 to provide an

* Corresponding author at: Department of Chemical Engineering, University of Waterloo, 200 University Avenue W, Waterloo, Ontario N2L 3G1, Canada. Tel.: +1 519 888 4567x38605; fax: +1 519 888 4347.
E-mail address: frank.gu@uwaterloo.ca (F.X. Gu).

http://dx.doi.org/10.1016/j.sbsr.2015.04.007
2214-1804/

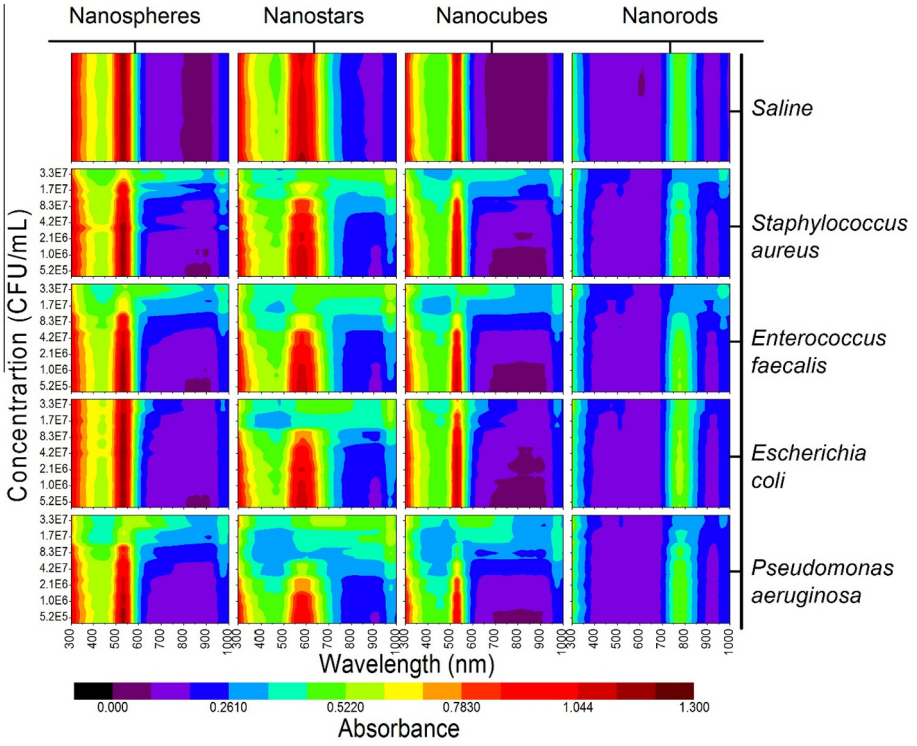

Fig. 1. UV–Visible absorption spectra of gold nanospheres, nanostars, nanocubes and nanorods in the presence of saline ($n = 12$) or bacteria ($n = 3$ per concentration) at various concentrations ranging from approximately 5.2×10^5 CFU/mL to 3.3×10^7 CFU/mL. Each of the saline plots is made up of 12 slices (one per replicate) and bacteria plots is made of 21 slices (three per concentration).

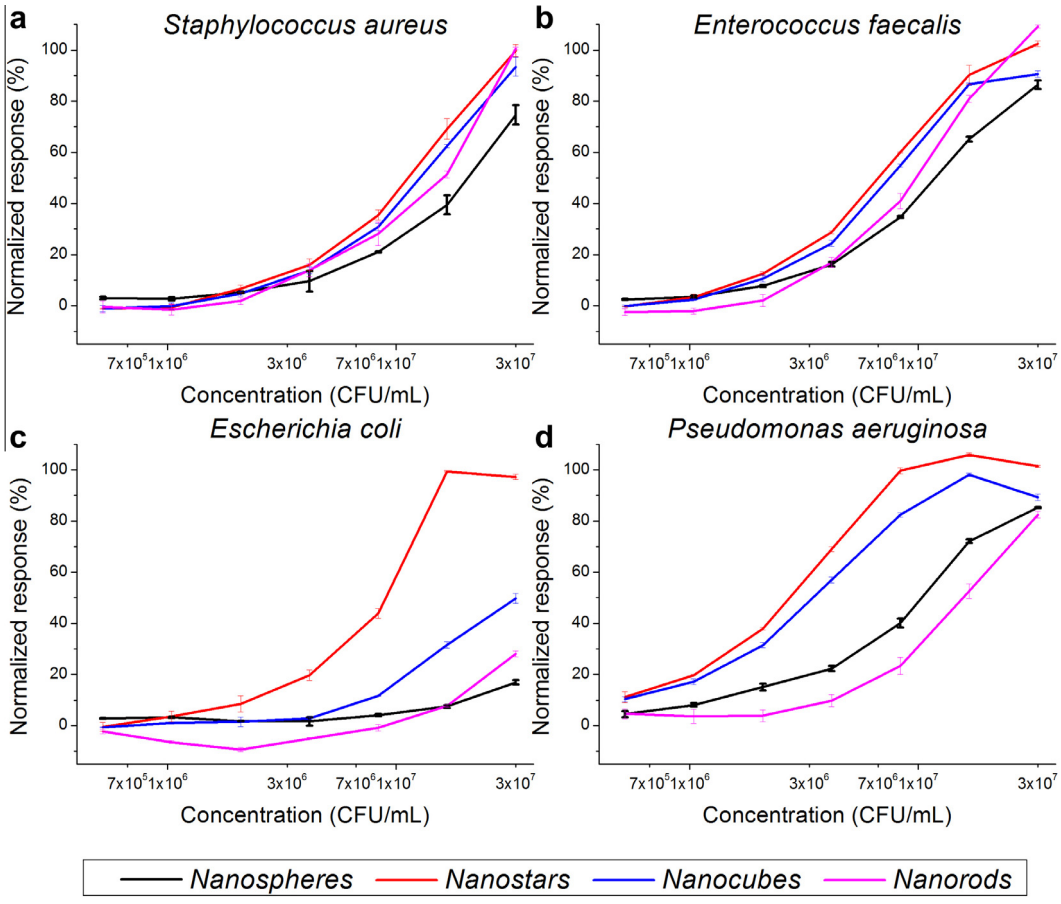

Fig. 2. Concentration dependent peak response obtained from (a) *Staphylococcus aureus*, (b) *Enterococcus faecalis*, (c) *Escherichia coli* and (d) *Pseudomonas aeruginosa* for different shapes of nanoparticles: nanospheres, nanostars, nanocubes, nanorods. Data is presented as mean ± S.D. ($n = 3$).

approximate concentration of 1×10^8 CFU/mL [13,17]. The bacteria were then serially diluted by a factor of two to obtain dilutions of $2x - 64x$. Then, 100 μL of each bacterial solution (eight concentrations and four species) was mixed with 200 μL of each gold nanoparticle solution in a 96-well microplate in triplicates. Saline was used as a control. The mixtures were incubated overnight and UV–Visible absorption spectra were obtained from 300 to 999 nm in increments of 1 nm. Further details of the experiments are provided in the Supplementary material.

3. Results and discussion

3.1. Spectrophotometric responses of each shape to different bacteria

The UV–Visible absorption spectra—plotted as contour plots in Fig. 1—show that the peak width, location, and intensity for each nanoparticle solution is different as indicated by the saline controls. The peak location is governed by the surface plasmon resonance frequency, which is unique for each shape of nanoparticle [18-20]. The peak width depends on the size and size distribution of the nanoparticles [21]. The intensity of absorption depends on the concentration and extinction coefficient of the nanoparticles [22,23]. Each of these qualities contributes to a characteristic spectrum for the various shapes of gold nanoparticles and thus adds responses for analysis in a "chemical nose" biosensor. When combined with bacteria, a colorimetric response is obtained due to the aggregation of the nanoparticles around the bacteria, caused by electrostatic interactions between cationic CTAB and anionic cell walls [5,6,13,24,25]. Fig. 1 exemplifies that the response from each bacterium is unique and distinct for different shapes of nanoparticles. While all bacteria present a concentration dependent response for each nanoparticle shape, the degree of response varies: *P. aeruginosa* provides the most change compared to saline and *E. coli* provides the least.

In order to quantify the response obtained among different nanoparticles and bacteria, the absorbance value at the peak (Table S1) was used and normalized against saline and baseline as explained in the Supporting material. The normalized response demonstrates that the shape of nanoparticles has minimal effect for Gram-positive bacteria but causes a drastic difference for Gram-negative bacteria (Fig. 2). Among all four bacteria, *P. aeruginosa* highlights the differences between nanoparticle shapes the most. Fig. 2d also shows that the response decreases in the following order: nanostars > nanocubes > nanospheres > nanorods.

Since the concentration of CTAB could be different for each nanoparticle solution, the effect of CTAB concentration on the response needs to be tested. We used gold nanostars as the model

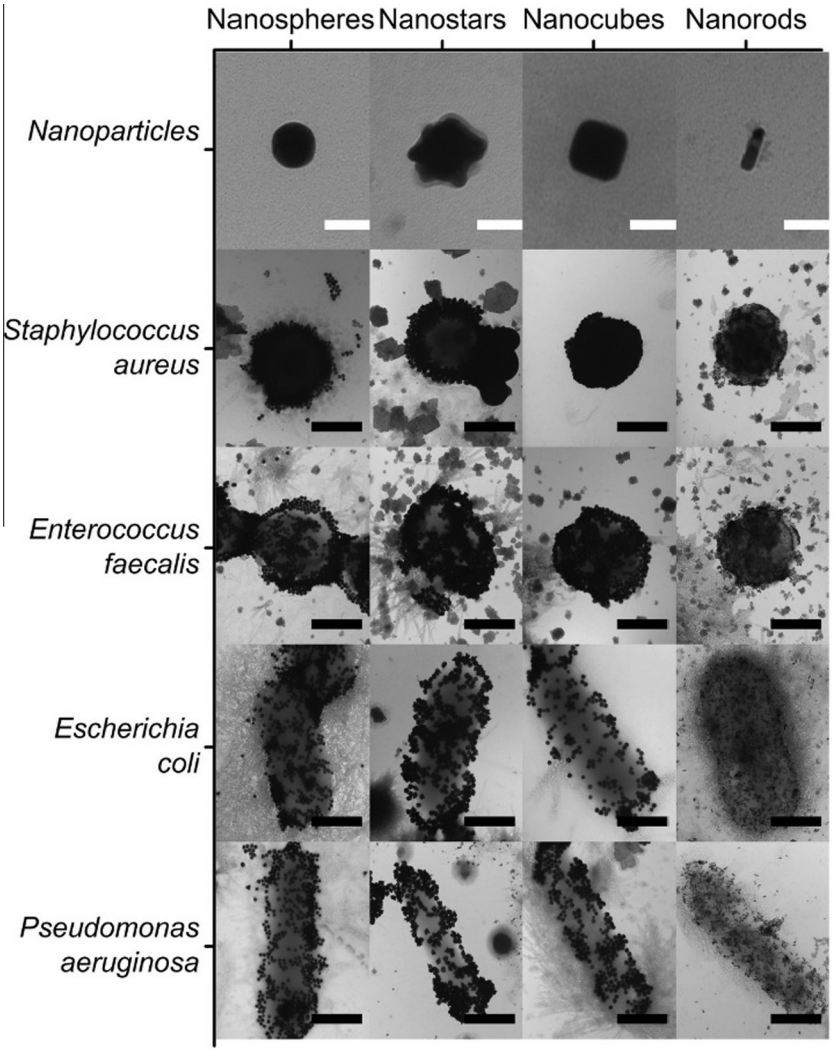

Fig. 3. Transmission electron microscopy (TEM) images of each of the different shapes of nanoparticles aggregating around various Gram-positive and Gram-negative bacteria. White scale bars are 50 nm and black scale bars are 500 nm.

nanoparticle and *S. aureus* as the model bacterium, while varying CTAB concentration from a range of 100 μM to 100 mM. The normalized response, reported in Fig. S1 (Supplementary material), does not depend on the concentration of CTAB. The differences in response for each shape seem to be dependent on the roughness of the nanoparticles, which would provide them a higher surface area and hence a higher area for interaction with bacterial cell walls. Additionally, particles with more branching (nanostars) or edges (cubes) are expected to be more protruding into the functional groups present on the bacterial surface [6].

3.2. Transmission electron microscopy

In order to obtain a better understanding of the aggregation of gold nanoparticles, TEM images were obtained for all bacteria-nanoparticle combinations. The TEM images show that the sizes of nanoparticles are comparable (Fig. 3). It is also observed that *S. aureus* and *E. faecalis* show complete coverage of the cell with nanospheres, nanostars, and nanocubes. In the case of nanorods, there are some areas that remain uncovered. Additionally, multilayer deposition is observed for *S. aureus*, which could be an indication of a higher extent of polyanionic teichoic acids [25-27] as compared to *E. faecalis*. In the case of Gram-negative bacteria, lipopolysaccharides and phospholipids are mostly responsible for the negative charge and hence the aggregation of cationic nanoparticles [5,6,28,29]. When looking at *E. coli*, a relatively uniform but sparse distribution of nanoparticles is observed for all shapes except nanostars, which is consistent with the colorimetric response observed in Fig. 2c. The TEM images of *P. aeruginosa* highlight an important behavior: the nanoparticles aggregate in specific areas of the bacterium as observed for the nanostars and nanocubes, while other sections of the surface are completely uncovered. The literature suggests that this localized aggregation would be due to the formation of lipid domains around specific proteins [30] or due to the addition of cationic molecules such as CTAB [31]. Specifically, anionic lipids such as phosphatidylglycerol and diphosphatidylglycerol (cardiolipin) would attract the nanoparticles and lead to aggregation. On the other hand, gold nanorods and nanospheres show a relatively uniform adsorption on the surface of the bacterium and also a lower response. This also suggests that if the lipid domains are responsible for selective aggregation, they might only be accessible via protruding nanoparticles.

To exclude the possibility that the differential responses observed for each type of nanoparticle were primarily due to their sizes instead of shapes, the colloidal stability of each nanoparticle solution was tested by comparing the absorbance in saline and Millipore water. If the response observed in the presence of bacteria was mainly a result of the size differences, it is expected that the nanoparticles would have decreasing colloidal stability and

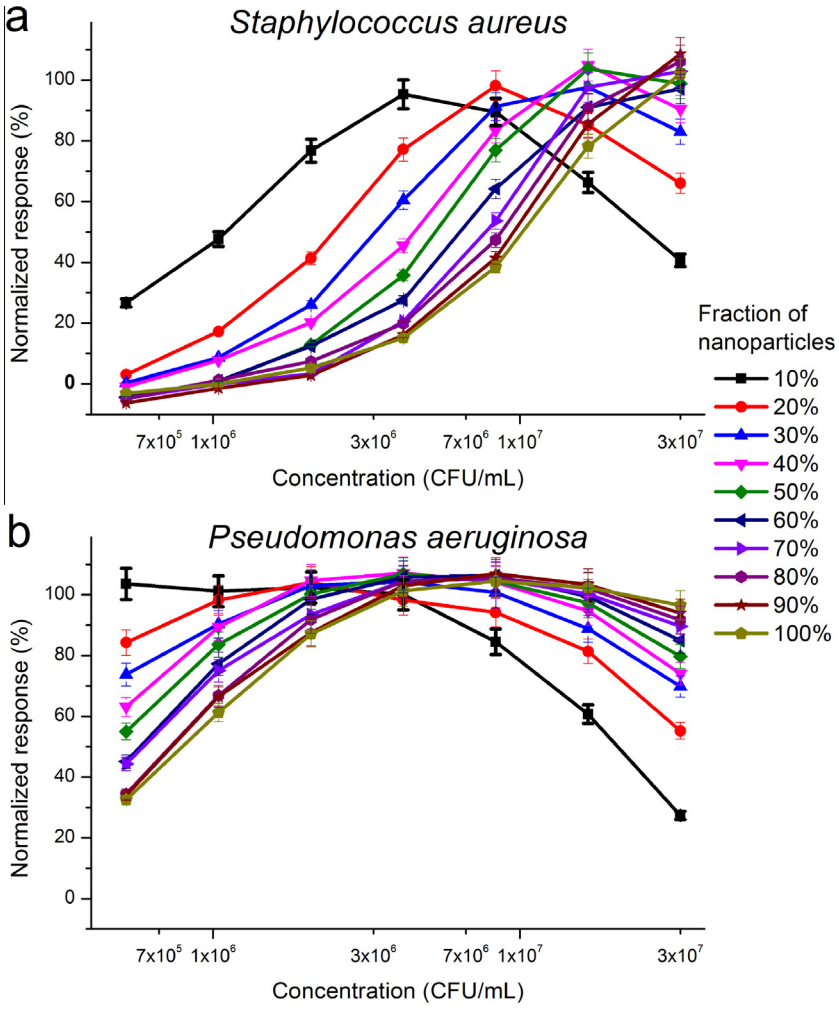

Fig. 4. The effect of nanoparticle concentration on colorimetric response for (a) Gram-positive *Staphylococcus aureus* and (b) Gram-negative *Pseudomonas aeruginosa*. Error bars are 5% of the normalized response values.

hence, lower peak absorbance values [13,32] in the following order: nanostars < nanocubes < nanospheres < nanorods. The results from the saline experiment are presented in Fig. S2 (Supplementary material) and they highlight that there is no correlation between the nanoparticle type and aggregation in saline. Thus, the bacterial response cannot be attributed to the small differences in the sizes of the various nanoparticles.

CTAB-coated nanoparticles can be used as a "chemical nose" by analyzing the response, developing a training set, and then matching the observed response of an unknown sample to the training set [6]. Since each nanoparticle shape provides a unique concentration-dependent curve for the same bacterium (Fig. 2c and d), this information can be used for increasing the specificity of the biosensor. This is possible if a mixture of shapes of nanoparticle is used. The mixture will have more features in the absorption spectrum as compared to a single nanoparticle solution in the form of peaks. Each of these additional peaks will respond differently to the bacteria present and thus serve as sources of independent responses to be analyzed for the "chemical nose." These additional responses will thus increase the number of bacteria that can be detected and identified. When considering the shape of nanoparticles for providing drastic responses, it is observed that nanostars provide the greatest response for all bacteria tested and hence should be used for applications requiring a visual color change, such as point-of-care detection.

3.3. The effect of nanoparticle concentration

An important strategy for altering the sensitivity and range of detection is to adjust the concentration of nanoparticles. We made linear dilutions of the stock gold nanostars in 1 mM CTAB to obtain a range of 10–100% fractions in increments of 10%. These fractions were then tested with various concentrations of *S. aureus* and *P. aeruginosa* and the normalized peak response is presented in Fig. 4. Interestingly, the concentration of nanostars has a greater impact on *S. aureus* as compared to *P. aeruginosa.* This could be because the concentrations tested for *P. aeruginosa* are already on the right side of the concentration-dependent response curve, where a saturation is observed. From the *S. aureus* samples, it is clear that the concentration of nanoparticles can be adjusted according to the bacteria concentration range of interest, where a lower fraction of nanoparticles is appropriate for a lower concentration of bacteria. This is because the colorimetric response is determined by the proportion of aggregated nanoparticles to non-aggregated nanoparticles. When there are fewer bacteria, this proportion is higher for a lower fraction of nanoparticles. Thus, lowering the concentration of nanoparticles provides a better detection limit and is ideal for applications requiring high sensitivity. On the other hand, a higher concentration of nanoparticles is preferred for visual detection of bacteria that have high infective doses and hence need to be detected a high concentration [33,34].

4. Conclusions

We have demonstrated that gold nanostars provide the most drastic response for a "chemical nose" biosensor and gold nanorods provide the least drastic. Different shapes of nanoparticles provide unique responses that can be analyzed to improve the specificity of a "chemical nose" biosensor. The concentration of nanoparticles can tune the detection limit and concentration range of bacteria that can be detected.

Conflict of interest

The authors declare no conflict of interest.

Acknowledgements

This work was financially supported by the Natural Sciences and Engineering Research Council of Canada (NSERC) and 20/20 NSERC – Ophthalmic Materials Network. M.S.V. is grateful for the NSERC Vanier Canada Graduate Scholarship. P.Z.C. is thankful for the NSERC Undergraduate Student Research Award. We would like to thank Jacob Rogowski and Erin Ellyse Bedford for proofreading and editing the manuscript.

Appendix A. Supplementary data

Supplementary data associated with this article can be found, in the online version, at http://dx.doi.org/10.1016/j.sbsr.2015.04.007.

References

[1] C.C. You, O.R. Miranda, B. Gider, P.S. Ghosh, I.B. Kim, B. Erdogan, et al., Detection and identification of proteins using nanoparticle-fluorescent polymer 'chemical nose' sensors, Nat. Nanotechnol. 2 (2007) 318–323.
[2] S.H. Lim, L. Feng, J.W. Kemling, C.J. Musto, K.S. Suslick, An optoelectronic nose for the detection of toxic gases, Nat. Chem. 1 (2009) 562–567.
[3] U.H. Bunz, V.M. Rotello, Gold nanoparticle-fluorophore complexes: Sensitive and discerning "noses" for biosystems sensing, Angew. Chem. Int. Ed. Engl. 49 (2010) 3268–3279.
[4] O.R. Miranda, X. Li, L. Garcia-Gonzalez, Z.J. Zhu, B. Yan, U.H. Bunz, et al., Colorimetric bacteria sensing using a supramolecular enzyme-nanoparticle biosensor, J. Am. Chem. Soc. 133 (2011) 9650–9653.
[5] R.L. Phillips, O.R. Miranda, C.C. You, V.M. Rotello, U.H. Bunz, Rapid and efficient identification of bacteria using gold-nanoparticle-poly(para-phenyleneethynylene) constructs, Angew. Chem. Int. Ed. Engl. 47 (2008) 2590–2594.
[6] M.S. Verma, P.Z. Chen, L. Jones, F.X. Gu, "Chemical nose" for the visual identification of emerging ocular pathogens using gold nanostars, Biosens. Bioelectron. 61 (2014) 386–390.
[7] Y. Wan, Y. Sun, P. Qi, P. Wang, D. Zhang, Quaternized magnetic nanoparticles-fluorescent polymer system for detection and identification of bacteria, Biosens. Bioelectron. 55 (2014) 289–293.
[8] O.R. Miranda, B. Creran, V.M. Rotello, Array-based sensing with nanoparticles: 'chemical noses' for sensing biomolecules and cell surfaces, Curr. Opin. Chem. Biol. 14 (2010) 728–736.
[9] M.S. Verma, J.L. Rogowski, L. Jones, F.X. Gu, Colorimetric biosensing of pathogens using gold nanoparticles, Biotechnol. Adv. (2015). in press.
[10] V. Rotello, Sniffing out cancer using "chemical nose" sensors, Cell Cycle 8 (2009) 3615–3616.
[11] K. Kusolkamabot, P. Sae-ung, N. Niamnont, K. Wongravee, M. Sukwattanasinitt, V.P. Hoven, Poly(N-isopropylacrylamide)-stabilized gold nanoparticles in combination with tricationic branched phenylene-ethynylene fluorophore for protein identification, Langmuir 29 (2013) 12317–12327.
[12] A. Bajaj, O.R. Miranda, I.B. Kim, R.L. Phillips, D.J. Jerry, U.H. Bunz, et al., Detection and differentiation of normal, cancerous, and metastatic cells using nanoparticle-polymer sensor arrays, Proc. Natl. Acad. Sci. U.S.A. 106 (2009) 10912–10916.
[13] M.S. Verma, P.Z. Chen, L. Jones, F.X. Gu, Branching and size of CTAB-coated gold nanostars control the colorimetric detection of bacteria, RSC Adv. 4 (2014) 10660–10668.
[14] H.W. Boucher, G.H. Talbot, J.S. Bradley, J.E. Edwards, D. Gilbert, L.B. Rice, et al., Bad bugs, no drugs: No ESKAPE! An update from the Infectious Diseases Society of America, Clin. Infect. Dis. 48 (2009) 1–12.
[15] W. Lu, A.K. Singh, S.A. Khan, D. Senapati, H. Yu, P.C. Ray, Gold nano-popcorn-based targeted diagnosis, nanotherapy treatment, and in situ monitoring of photothermal therapy response of prostate cancer cells using surface-enhanced Raman spectroscopy, J. Am. Chem. Soc. 132 (2010) 18103–18114.
[16] H. Ahn, H. Lee, K. Jin, K.T. Nam, Extended gold nano-morphology diagram: Synthesis of rhombic dodecahedra using CTAB and ascorbic acid, J. Mater. Chem. C 1 (2013) 6861–6868.
[17] J. Dantam, H. Zhu, F. Stapleton, Biocidal efficacy of silver-impregnated contact lens storage cases in vitro, Invest. Ophthalmol. Vis. Sci. 52 (2011) 51–57.
[18] K. Kelly, E. Coronado, L. Zhao, G. Schatz, The optical properties of metal nanoparticles: The influence of size, shape, and dielectric environment, J. Phys. Chem. B 107 (2003) 668–677.
[19] M.A. El-Sayed, Some interesting properties of metals confined in time and nanometer space of different shapes, Acc. Chem. Res. 34 (2001) 257–264.
[20] Y. Xia, Y. Xiong, B. Lim, S.E. Skrabalak, Shape-controlled synthesis of metal nanocrystals: simple chemistry meets complex physics?, Angew. Chem. Int. Ed. Engl. 48 (2009) 60–103.
[21] H. Yuan, C.G. Khoury, H. Hwang, C.M. Wilson, G.A. Grant, T. Vo-Dinh, Gold nanostars: Surfactant-free synthesis, 3D modelling, and two-photon photoluminescence imaging, Nanotechnology 23 (2012) (075102–4484/23/7/075102, Epub 2012 Jan 20).

[22] P.K. Jain, K.S. Lee, I.H. El-Sayed, M.A. El-Sayed, Calculated absorption and scattering properties of gold nanoparticles of different size, shape, and composition: Applications in biological imaging and biomedicine, J. Phys. Chem. B 110 (2006) 7238–7248.
[23] X. Liu, M. Atwater, J. Wang, Q. Huo, Extinction coefficient of gold nanoparticles with different sizes and different capping ligands, Colloids Surf., B Biointerfaces 58 (2007) 3–7.
[24] S.C. Hayden, G. Zhao, K. Saha, R.L. Phillips, X. Li, O.R. Miranda, et al., Aggregation and interaction of cationic nanoparticles on bacterial surfaces, J. Am. Chem. Soc. 134 (2012) 6920–6923.
[25] V. Berry, A. Gole, S. Kundu, C.J. Murphy, R.F. Saraf, Deposition of CTAB-terminated nanorods on bacteria to form highly conducting hybrid systems, J. Am. Chem. Soc. 127 (2005) 17600–17601.
[26] V. Berry, R.F. Saraf, Self-assembly of nanoparticles on live bacterium: An avenue to fabricate electronic devices, Angew. Chem. Int. Ed. Engl. 44 (2005) 6668–6673.
[27] W.W. Navarre, O. Schneewind, Surface proteins of gram-positive bacteria and mechanisms of their targeting to the cell wall envelope, Microbiol. Mol. Biol. Rev. 63 (1999) 174–229.
[28] J. Sun, J. Ge, W. Liu, X. Wang, Z. Fan, W. Zhao, et al., A facile assay for direct colorimetric visualization of lipopolysaccharides at low nanomolar level, Nano Res. 5 (2012) 486–493.
[29] Y. Hong, D.G. Brown, Cell surface acid-base properties of Escherichia coli and Bacillus brevis and variation as a function of growth phase, nitrogen source and C:N ratio, Colloids Surf., B Biointerfaces 50 (2006) 112–119.
[30] K. Matsumoto, J. Kusaka, A. Nishibori, H. Hara, Lipid domains in bacterial membranes, Mol. Microbiol. 61 (2006) 1110–1117.
[31] R.M. Epand, R.F. Epand, Lipid domains in bacterial membranes and the action of antimicrobial agents, Biochim. Biophys. Acta 1788 (2009) 289–294.
[32] G. Zhang, Z. Yang, W. Lu, R. Zhang, Q. Huang, M. Tian, et al., Influence of anchoring ligands and particle size on the colloidal stability and in vivo biodistribution of polyethylene glycol-coated gold nanoparticles in tumor-xenografted mice, Biomaterials 30 (2009) 1928–1936.
[33] D. Dutta, M.D. Willcox, Antimicrobial contact lenses and lens cases: A review, Eye Contact Lens 40 (2014) 312–324.
[34] P. Schmid-Hempel, S.A. Frank, Pathogenesis, virulence, and infective dose, PLoS Pathog. 3 (2007) 1372–1373.